CORE

Metadata, citation and similar papers at core.ac.uk

Provided by Radboud Repository

Radboud Repository

Radboud University Nijmegen

PDF hosted at the Radboud Repository of the Radboud University Nijmegen

The following full text is a publisher's version.

For additional information about this publication click this link.
http://hdl.handle.net/2066/130384

Please be advised that this information was generated on 2017-12-05 and may be subject to change.

THE JOURNAL OF BIOLOGICAL CHEMISTRY VOL. 281, NO. 51, pp. 39561–39572, December 22, 2006
© 2006 by The American Society for Biochemistry and Molecular Biology, Inc. Printed in the U.S.A.

$P2X_5$ Subunit Assembly Requires Scaffolding by the Second Transmembrane Domain and a Conserved Aspartate*

Received for publication, June 26, 2006, and in revised form, September 6, 2006 Published, JBC Papers in Press, September 25, 2006, DOI 10.1074/jbc.M606113200

Wiebke Duckwitz, Ralf Hausmann, Armaz Aschrafi[1], and Günther Schmalzing[2]
From the Department of Molecular Pharmacology, Rheinisch-Westfaelische Technische Hochschule (RWTH) Aachen, Wendlingweg 2, D-52074 Aachen, Germany

Functional homomeric and heteromeric ATP-gated P2X receptor channels have been shown to display a characteristic trimeric architecture. Of the seven different isoforms (designated $P2X_1$-$P2X_7$), $P2X_5$ occurs in humans primarily as a nonfunctional variant lacking the C-terminal end of the ectodomain and the outer half of the second transmembrane domain. We show that this truncated variant, which results from the splice-skipping of exon 10, is prone to subunit aggregation because the residual transmembrane domain 2 is too short to insert into the membrane. Alleviation of the negative hydrophobic mismatch by the addition of a stretch of moderately hydrophobic residues enabled formation of a second membrane-spanning domain and strictly parallel homotrimerization. Systematic mutagenesis identified only one transmembrane domain 2 residue, Asp^{355}, which supported homotrimerization in a side chain-specific manner. Our results indicate that transmembrane domain 2 formation contributes 2-fold to $hP2X_5$ homotrimerization by tethering the end of the ectodomain to the membrane, thereby topologically restricting conformational mobility, and by intramembrane positioning of Asp^{355}. While transmembrane domain 2 appears to favor assembly by enabling productive subunit interactions in the ectodomain, Asp^{355} seems to assist by simultaneously driving intramembrane helix interactions. Overall, these results indicate a complex interplay between topology, helix-helix interactions, and oligomerization to achieve a correctly folded structure.

P2X receptors comprise a family of ligand-gated ion channels that are activated by extracellular ATP and mediate rapid signaling in a large variety of cells including neurons, smooth and cardiac muscles, epithelia, and lymphocytes (1). Seven subunit isoforms, designated $P2X_1$-$P2X_7$, have been identified and share a common topology with cytosolic N- and C-terminal domains and two membrane-spanning regions (transmembrane (TM) 1 and TM2)[3] connected by a large *N*-glycosylated ectodomain comprising 10 conserved cysteine residues. Like all other known ligand-gated ion channels, P2X receptors are oligomers of identical (homomeric) or homologous (heteromeric) subunits. Biochemical (2–4), biophysical (5), and functional studies (6) revealed that a trimeric architecture driven by noncovalent intermolecular interactions is a structural hallmark of functional homomeric and heteromeric P2X receptors. The three subunits are thought to arrange circularly, contributing one or both transmembrane domains to form a central cation-conducting pore.

The assembly pathway leading to this trimeric structure is not well characterized. The question of which molecular determinants lead to the assembly of subunits into P2X receptors has so far been addressed by examining the ability of deletion mutants and chimeric constructs to associate with full-length P2X subunits in a co-immunoprecipitation assay (7). Neither the N- nor C-terminal cytoplasmic domain was found to be important for assembly. However, a deletion mutant terminating 25 amino acids before the start of the TM2 domain was unable to interact with either of the wild type subunits or with itself. This suggested that either TM2 or a region immediately upstream of TM2 carried a critical determinant of specific subunit-subunit interactions, although the possibility that the lack of co-assembly was the result of an inadequate secondary or tertiary structure was not ruled out (7).

To further examine the role of both TM2 and the pre-TM2 region in P2X receptor assembly, we utilized the $P2X_5$ isoform, which occurs in humans predominantly as a natural deletion mutant (designated $hP2X_5^{\Delta 328-349}$) and lacks much of the TM2 and pre-TM2 regions as a result of the splicing-out of exon 10 (8). The $hP2X_5^{\Delta 328-349}$ cDNA does not encode functional channels, but a receptor chimera consisting of the N-terminal and C-terminal halves of the human and the rat $P2X_5$ subunits, respectively, has been expressed in *Xenopus laevis* oocytes and is functional (8). A full-length $hP2X_5$ subunit generated by incorporating a sequence corresponding to exon 10 (as identified by a TBLASTN search of human genomic DNA) was expressed well in human embryonic kidney 293 cells and provided robust ATP-dependent currents (9). In this report we sequentially generated a full-length $hP2X_5$ subunit cDNA by progressively and repeatedly inserting codons for 4–8 amino acids of the spliced-out exon 10 and then determined the assembly state of the resultant constructs by blue native PAGE. We also challenged homotrimerization of the full-length $P2X_5$ subunit by block replacements of amino acids throughout the pre-TM2 and TM2 regions to test for the presence of residues important for $P2X_5$ subunit-subunit recognition. Our results

---

* This work was supported by Deutsche Forschungsgemeinschaft Grants Schm 536/6 and Schm536/7 (to G. S.) and by the START-Program of the Faculty of Medicine, RWTH Aachen University (to R. H.). The costs of publication of this article were defrayed in part by the payment of page charges. This article must therefore be hereby marked "*advertisement*" in accordance with 18 U.S.C. Section 1734 solely to indicate this fact.

[1] Present address: Section on Molecular Neurobiology, Laboratory of Molecular Biology, National Institute of Mental Health, Bldg. 10, Rm. 4D14, 10 Center Dr., Bethesda, MD 20892

[2] To whom correspondence should be addressed. Tel.: 49-241-8089130; Fax: 49-241-8082433; E-mail: gschmalzing@ukaachen.de.

[3] The abbreviations used are: TM, transmembrane; NTA, nitrilotriacetic acid; h- human; r-, rat; Tricine, *N*-[2-hydroxy-1,1-bis(hydroxymethyl)ethyl]glycine; WT, wild type.

are consistent with the view that TM2 supports homotrimerization in a relatively sequence-unspecific manner by tethering the C-terminal end of the large ectodomain to the membrane; thus, by defining the overall shape of the ectodomain, TM2 spatially constrains folding events in a productive way. We detected a specific role in assembly recognition for only one TM2 residue, Asp^{355}, which is fully conserved among P2X family members and may stabilize helix-helix interactions by satisfying hydrogen bonding groups in the membrane.

MATERIALS AND METHODS

P2X cDNA Constructs—To indicate the species origin, P2X subunit names are preceded by "h" or "r" for human or rat, respectively. Constructs from previous work include His-rP2X$_1$ (2) and His-rP2X$_5$ (4), which encode the rat P2X$_1$ and P2X$_5$ subunit with N-terminal His tags. The original rP2X$_5$ clone was kindly provided by Dr. Florentina Soto (10). A cDNA encoding the hP2X$_5$ subunit (GenBank™ accession number AAC51931 (8)) was isolated by PCR from a human brain cDNA library (Invitrogen) using sequence-specific primer pairs (forward, aaagaattcCATGGGGCAGGCGGGCTGCAA; reverse, aaagaattcGAGGCAATTCACGTGCTCCTGTGGGGCT; EcoRI cloning sites are underlined) subcloned into the oocyte expression vector pNKS2 (11) and entirely sequenced. Codon insertions and replacement mutations were introduced by QuikChange site-directed mutagenesis (Stratagene, La Jolla, CA).

P2X Receptor Expression in X. laevis Oocytes—Defolliculated *X. laevis* oocytes injected with capped cRNAs as described previously (12) were kept at 19 °C in sterile frog Ringer's solution (ORi: 90 mM NaCl, 1 mM KCl, 1 mM CaCl$_2$, 1 mM MgCl$_2$, and 10 mM Hepes, pH 7.4) supplemented with 50 μg/ml gentamycin. Two days after cRNA injection, ATP responses were measured by two-electrode voltage-clamp recording at a holding potential of −60 mV as described previously (13). Capping the N-terminal end of the rP2X$_5$ subunit with a His tag for one-step affinity purification had virtually no effect on the electrophysiological phenotype of the corresponding receptor in *X. laevis* oocytes (results not shown).

Radiolabeling and Affinity Purification of P2X$_5$ Receptor Constructs—For metabolic radiolabeling, cRNA-injected oocytes and non-injected controls were incubated overnight with L-[^{35}S]methionine (>40 TBq/mmol, Amersham Biosciences) at about 100 MBq/ml (0.4 MBq per oocyte) in ORi at 19 °C and then chased for 24 h. His-tagged receptors were purified by Ni^{2+}-nitrilotriacetic acid (NTA)-agarose (Qiagen, Hilden, Germany) chromatography from digitonin (1.0%) extracts of oocytes as detailed previously (2, 14). Proteins were eluted from Ni^{2+}-NTA-agarose with non-denaturing buffer consisting of 250 mM imidazole/HCl, pH 7.4, and 1% digitonin (buffer 1) and then kept at 0 °C until analysis, which was carried out on the same day as purification.

P2X$_5$ receptor constructs at the plasma membrane were selectively labeled by incubating oocytes 2 days after cRNA injection with ^{125}I-labeled sulfosuccinimidyl-3-(4-hydroxyphenyl)propionate, a membrane-impermeant derivative of the Bolton-Hunter reagent (15) exactly as described previously (2, 4). Proteins were purified from digitonin extracts of the oocytes by Ni^{2+}-NTA-agarose chromatography as detailed above.

Trypsin Resistance Assay—P2X$_5$ receptor constructs, purified by non-denaturing Ni^{2+} affinity chromatography, were treated with 10–1000 μg/ml of bovine trypsin (Sigma-Aldrich) for 15 min on ice in buffer 1. Reactions were terminated by the addition of a 5-fold excess of soybean trypsin inhibitor. Digested samples were then analyzed by Tricine-SDS-PAGE with PhosphorImager scanning (see below).

Blue Native PAGE and SDS-PAGE—Blue native PAGE (16, 17) was carried out as described (2) using gradient gels (4–20% acrylamide). For partial dissociation of natively purified P2X receptors into lower-order complexes down to monomers, samples were treated for 1 h at 37 °C with 0.1% SDS or 4–8 M urea as indicated. For SDS-PAGE or Tricine-SDS-PAGE (18), proteins were supplemented with the appropriate SDS-PAGE sample buffer containing 20 mM dithiothreitol followed by heating to 56 °C for 15 min and electrophoresed in parallel with ^{14}C-labeled molecular mass markers (Rainbow™, Amersham Biosciences). In some experiments samples were treated before SDS-PAGE for 2 h at 37 °C with either endoglycosidase H or peptide:*N*-glycosidase F (PNGase F) (New England Biolabs, Frankfurt, Germany) in the presence of 1% Nonidet P-40 to decrease inactivation of PNGase F. Both SDS-PAGE gels and blue native PAGE gels were fixed, dried, exposed to a PhosphorImager screen, and scanned using a Storm 820 PhosphorImager (Amersham Biosciences). Individual bands were quantified with the ImageQuant software.

RESULTS

Functional Rat P2X$_5$ Receptors Possess a Homotrimeric Architecture—All P2X$_5$ constructs in this study were N-terminal-tagged with a hexahistidyl sequence to allow for protein purification by metal affinity chromatography after expression in *X. laevis* oocytes. Oocytes expressing WT rP2X$_5$ subunits or His-rP2X$_5$ subunits responded to ATP with a non-desensitizing inward current of similar shape and magnitude. A typical current trace in response to ATP from His-rP2X$_5$ subunit-expressing oocytes is shown in Fig. 1*A*. The shape of the current trace was notably changed when rP2X$_5$ receptors were repeatedly challenged with ATP. We observed the development of a slowly activating inward current, which was most likely mediated by secondary activation of oocyte endogenous channels since it was greatly reduced by flufenamic acid, an inhibitor of Ca^{2+}-activated Cl$^-$ channels (19). Flufenamic acid did not affect the shape of the current component attributable to the ATP-activated rP2X$_5$ channel (results not shown).

We have previously demonstrated that the blue native PAGE technique has the capacity to correctly display the quaternary state of receptor channels and transporters. These include the known pentameric structure of Cys-loop receptors (2, 20–22) and the trimeric structure of glutamate transporters (23), which has also been visualized by x-ray crystallography (24). Like other oocyte-expressed P2X receptors except for hP2X$_6$ (4), the plasma membrane-bound rP2X$_5$ receptor migrated on the blue native PAGE gel as a distinct protein band (Fig. 1*B*, *lane 1*). Treatment with urea (*lanes* 2 and *3*) resulted in a ladder-like pattern of three bands, each separated by the approximate mass of an rP2X$_5$ monomer. Using this ladder as a mass marker, a trimeric state can be assigned to the non-denatured rP2X$_5$ receptor.

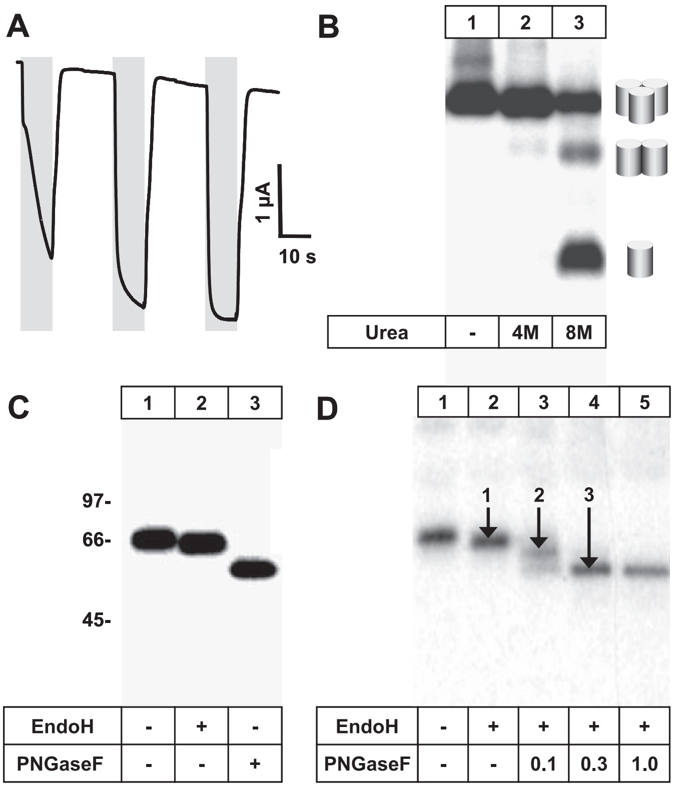

FIGURE 1. **Electrophysiological and biochemical analysis of rP2X$_5$ receptors expressed in *X. laevis* oocytes.** *A*, a typical current trace elicited by three subsequent applications of 10 μM ATP (denoted by *gray areas*) in 30-s intervals. The superfusion solution was supplemented with 0.1 mM flufenamic acid to suppress activation of endogenous chloride channels. *B*, His-rP2X$_5$ subunit-expressing oocytes were surface-radioiodinated with ^{125}I-labeled sulfosuccinimidyl-3-(4-hydroxyphenyl)propionate before receptor purification by non-denaturing Ni^{2+}-NTA chromatography. Migration of the plasma membrane-bound P2X$_5$ receptor on a blue native PAGE gel is shown both in the non-denatured homotrimeric state and in the partially denatured state (produced by a 1-h treatment at 37 °C with urea in concentrations as indicated). The barrels schematically illustrate trimeric, dimeric, and monomeric states. *C*, the same samples as in *B* were deglycosylated by endoglycosidase H (*EndoH*) or peptide:*N*-glycosidase F (*PNGase F*) as indicated and analyzed by SDS-PAGE. *D*, after removal of the single high mannose-type glycan with endoglycosidase H (indicated by *arrow 1*), further deglycosylation with increasing concentrations of peptide:*N*-glycosidase F yielded a glycosylated intermediate (*arrow 2*) and the fully deglycosylated rP2X$_5$ subunit (*arrow 3*).

Plasma membrane-bound rP2X$_5$ subunits bear three *N*-glycans, which add ~10 kDa of carbohydrate to the protein core (Fig. 1*C*). The mass calculated from the protein sequence is 52 kDa including the His tag, which is in good agreement with the experimental mass of ~54 kDa of the fully deglycosylated protein. The different glycosylated states obtained by combined deglycosylation with endoglycosidase H and submaximally effective concentrations of peptide:*N*-glycosidase F indicate that all three predicted *N*-glycosylation sites (^{77}NTT, ^{157}NST, ^{202}NFS) were occupied, one with a high mannose-type glycan and two with complex-type glycans (Fig. 1*D*).

Human P2X$_5$ Subunits Lacking Exon 10 Are Trimerization-defective—Using gene-specific primer pairs, we PCR-amplified an hP2X$_5$ cDNA from a human brain cDNA library. The deduced amino acid sequence was identical to a previously reported hP2X$_5$ splice variant that lacked exon 10 (8). We refer to this splice variant as hP2X$_5^{\Delta328-349}$ to indicate that codons 328–349 of the full-length P2X$_5$ subunit are missing. The location of the exon 10-specified sequence relative to the membrane is schematically illustrated in Fig. 2*A*.

Consistent with previous studies (8), expression of hP2X$_5^{\Delta328-349}$ in *Xenopus* oocytes did not lead to the formation of an ATP-gated cation channel. Because trimerization is essential for P2X receptor function, we performed a blue native PAGE analysis to investigate the assembly status of this splice variant. Fig. 2*B*, *lane 1*, shows that the [^{35}S]methionine-labeled His-hP2X$_5^{\Delta328-349}$ protein was poorly expressed and migrated on the blue native PAGE gel as an amorphous mass of protein (indicative of aggregates) rather than as a distinct band. In contrast, full-length His-rP2X$_5$ subunits migrated largely as homotrimers (Fig. 2*B*, *lanes 10* and *11*). We conclude that the lack of exon 10 results in a severe assembly defect that prevents the formation of functional homotrimeric hP2X$_5$ receptor channels at the level of subunit assembly in the endoplasmic reticulum.

Not All Exon 10-Encoded Residues Are Necessary for the Trimerization and Plasma Membrane Localization of hP2X$_5$ Subunits—To examine which of the 22 amino acids encoded by exon 10 were necessary for proper trimer formation and ion channel function, we progressively rebuilt exon 10 by inserting codons for 4–8 consecutive amino acids at a time, thus generating by stages a full-length hP2X$_5$ subunit cDNA (Fig. 2*B*). The inserted codons correspond to those previously identified by a TBLAST search of human genomic DNA corresponding to exon 10 (9). Expression of the various hP2X$_5$ constructs in *X. laevis* oocytes revealed that insertion of a minimum of 11 amino acids (residues 328–338; construct 3) from the total of 22 amino acids encoded by exon 10 was required to mediate significant homotrimer formation.

Trimerization was associated with increased protein stability and with plasma membrane localization of properly assembled trimers (Fig. 2*D*) but not with the formation of a functional receptor channel (Fig. 2*C*). ATP-gated inward currents could be elicited only from oocytes expressing the full-length His-hP2X$_5$ subunit (Fig. 2*C*, *lane 8*). The trimerization-defective constructs His-hP2X$_5^{\Delta328-349}$ and His-hP2X$_5^{\Delta335-349}$ were neither functional (Fig. 2*C*, *lanes 1* and *2*) nor exported to the cell surface (Fig. 2*D*, *lane 2*). Accordingly, once the span of inserted residues specified by exon 10 is of adequate length to allow for trimer formation, the resultant protein complex must have a sufficiently native-like conformation to be no longer recognized and retained by the endoplasmic reticulum quality control system, which retains malfolded proteins.

Insertion of Alanines, but Not Serines, Supports Trimerization as Efficiently as the Insertion of Genuine Exon 10 Residues—Insertion of seven residues, ^{335}PTIINVG^{341}, into the His-hP2X$_5^{\Delta335-349}$ construct resulted in a polypeptide that efficiently assembled into homotrimers (*cf.* Fig. 2*B*, *lane 4*). To determine whether this effect was sequence specific, we inserted a stretch of seven alanine or serine residues instead of the genuine ^{335}PTIINVG^{341} sequence and examined whether any of these substitutions was able to support oligomerization (Fig. 2*B*). Strikingly, the polyalanine stretch (*lane 5*) supported trimerization equally well as the ^{335}PTIINVG^{341} sequence, whereas the polyserine stretch (*lane 6*) did not.

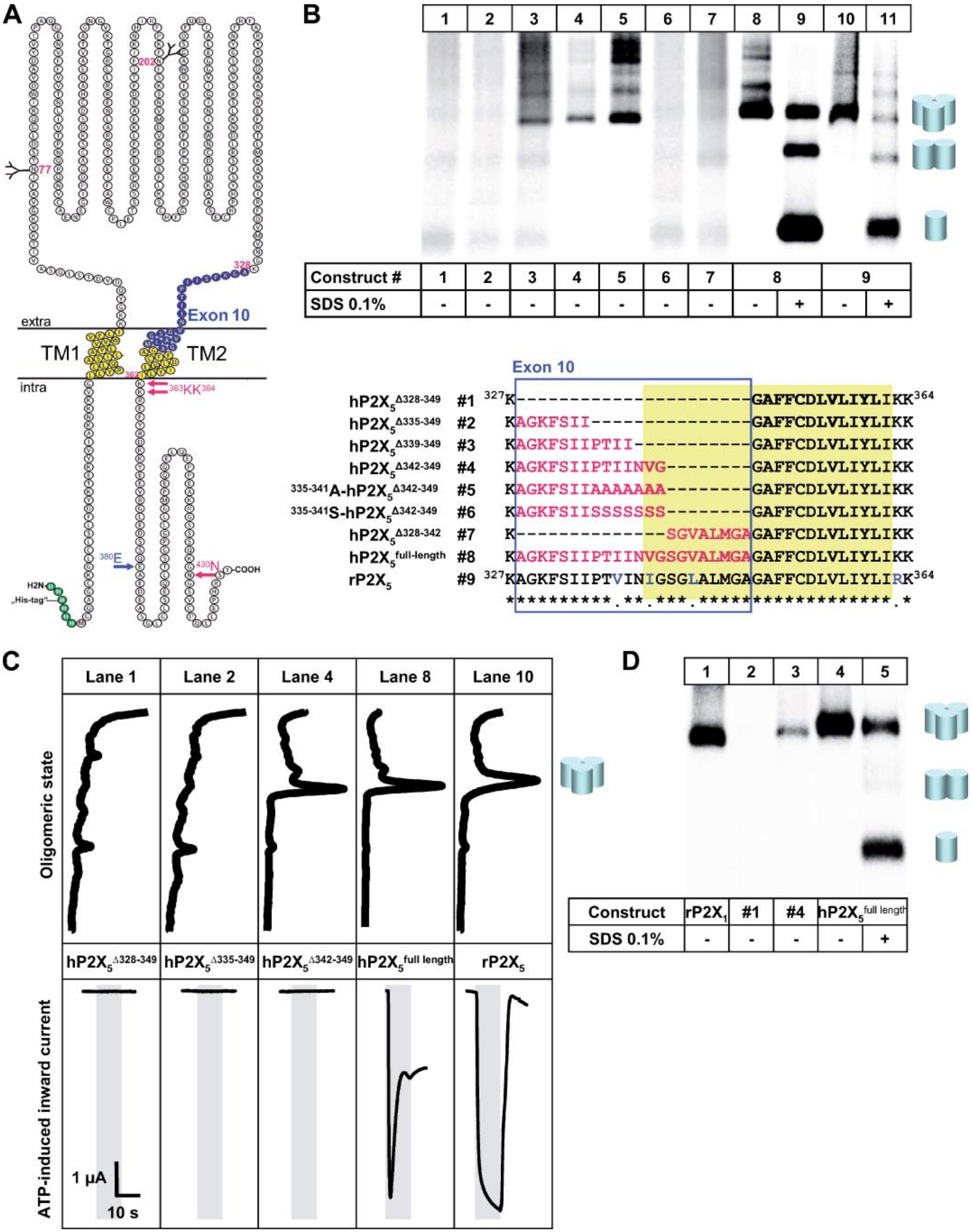
A
202
77
328
Exon 10
extra
TM1
TM2
intra
362
363KK364
380E
430N
H2N-
„His-tag"
-COOH
B
1 2 3 4 5 6 7 8 9 10 11
Construct # 1 2 3 4 5 6 7 8 9
SDS 0.1% - - - - - - - - + - +
Exon 10
hP2X5Δ328-349 #1 327K-----------------------GAFFCDLVLIYLIKK364
hP2X5Δ335-349 #2 KAGKFSII---------------GAFFCDLVLIYLIKK
hP2X5Δ339-349 #3 KAGKFSIIPTII-----------GAFFCDLVLIYLIKK
hP2X5Δ342-349 #4 KAGKFSIIPTIINVG--------GAFFCDLVLIYLIKK
335-341A-hP2X5Δ342-349 #5 KAGKFSIIAAAAAAA--------GAFFCDLVLIYLIKK
335-341S-hP2X5Δ342-349 #6 KAGKFSIISSSSSSS--------GAFFCDLVLIYLIKK
hP2X5Δ328-342 #7 K--------------SGVALMGAGAFFCDLVLIYLIKK
hP2X5full-length #8 KAGKFSIIPTIINVGSGVALMGAGAFFCDLVLIYLIKK
rP2X5 #9 327KAGKFSIIPTVINIGSGLALMGAGAFFCDLVLIYLIRK364
**********.**.***.*****************.*
C
Lane 1
Lane 2
Lane 4
Lane 8
Lane 10
Oligomeric state
hP2X5Δ328-349
hP2X5Δ335-349
hP2X5Δ342-349
hP2X5full length
rP2X5
ATP-induced inward current
1 µA
10 s
D
1 2 3 4 5
Construct rP2X1 #1 #4 hP2X5full length
SDS 0.1% - - - - +

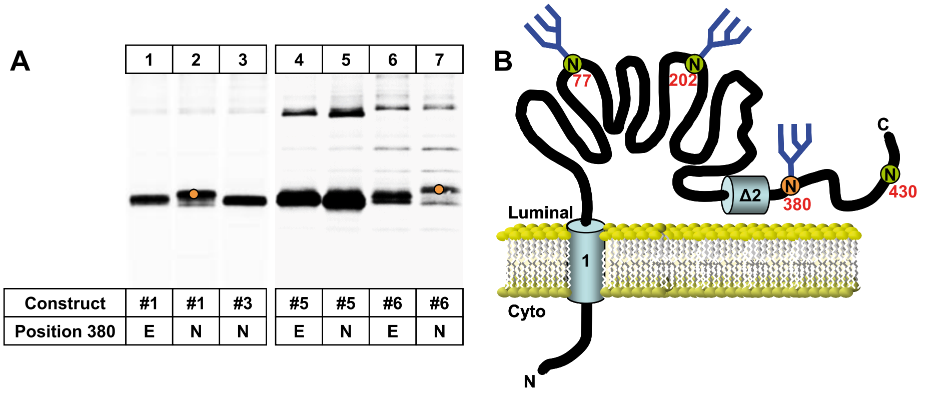

FIGURE 3. **A hydrophobic mismatch prevents formation of a second transmembrane domain.** *A*, PhosphorImager scan of an SDS-PAGE gel. Where indicated, the wild type residue Glu^{380} was replaced by Asn to generate a glycosylation reporter site (^{380}NDS) 65 residues from the C-terminal end. Construct numbers are the same as those used in Fig. 2. Triply glycosylated protein bands are indicated by an *orange dot*. *B*, topology schematic illustrating the position of natural glycosylation acceptor sites (*green circles*) and the engineered reporter site (*orange circle*). If two membrane-spanning domains are formed, only the two natural sites ^{77}NTS and ^{202}NFS are accessible for *N*-glycosylation. The third natural glycosylation site, ^{430}NGS, is too close to the C-terminal end to be used if topologically accessible.

Trimerization Parallels the Formation of a Second Membrane-spanning Segment—A possible explanation of these results is that alanine but not serine residues are capable of complementing the missing outer portion of TM2, thus allowing for membrane anchoring of the C-terminal end of the ectodomain. To address this possibility, we tried to exploit the fact that the hP2X$_5$ subunit carries an *N*-glycosylation sequence, ^{430}NGS (numbering refers to the full-length hP2X$_5$ subunit), which is normally topologically inaccessible because it resides on the C-terminal endodomain (*cf.* topology model in Fig. 2*A*). This site may be expected to be *N*-glycosylated when TM2 is excluded from the lipid bilayer, thus forcing the C-terminal tail to remain aberrantly located in the endoplasmic reticulum lumen. Deglycosylation analysis, however, provided no evidence for hyperglycosylation of the hP2X$_5$$^{\Delta 328-349}$ polypeptide, which could be shown to carry two *N*-glycans (results not shown); this is fully consistent with the occurrence of two *N*-glycosylation sites in the ectodomain.

^{430}NGS may remain unused as an acceptor site because of its short distance of only 15 residues to the C-terminal end (25). Therefore, we mutated the normally cytoplasmic Glu^{380} to Asn, thus generating an artificial glycosylation reporter sequence (^{380}NDS; numbering refers to the full-length hP2X$_5$ subunit) located at a more distal position of 65 residues from the C-terminal end. Fully efficient glycosylation has been shown to occur if 60 or greater residues separate the glycosylation acceptor site from the C terminus (25). Indeed, the corresponding hP2X$_5$$^{\Delta 328-349}$ mutant migrated with a 2–3-kDa higher mass (Fig. 3*A*, *lane 2*) than the parent construct (*lane 1*), demonstrating glycosylation of Asn^{380} and, hence, a luminal orientation of most likely the entire C-terminal tail (*cf.* model in Fig. 3*B*). This result can best be reconciled with the exclusion of the incomplete TM2 sequence Gly^{350}–Ile^{362} from the membrane as a result of a negative hydrophobic mismatch that occurs when the length of a hydrophobic transmembrane segment is too short to span the thickness of the hydrophobic bilayer (26). This is supported by the observation that the identical acceptor site remained unused when engineered into the trimerization-competent hP2X$_5$$^{\Delta 339-349}$ construct (Fig. 3*A*, *lane 3*). Evidently, pre-TM2 residues Ala^{328}–Ile^{338} can combine with the TM2-authentic residues Gly^{350}–Ile^{362} to form a hydrophobic domain of sufficient length to be integrated into the membrane. The concurrency of correct transmembrane threading and appearance of homotrimers on the blue native PAGE gel suggests an important role for TM2 in P2X$_5$ subunit homotrimerization.

Hydrophobicity of TM2 and of TM2-embedded Aspartate 355 Contributes to Stable hP2X$_5$ Homotrimer Formation—To further examine the contribution of amino acid side chains specified by exon 10 and more distal sequences to trimerization in the context of the full-length hP2X$_5$, we carried out a systematic mutagenesis. Five consecutive amino acids were replaced by single alanines throughout the sequence Lys^{330}–Leu^{361} (except for one double alanine mutation, ^{328}AGKF^{331} to ^{328}AGAA^{331}) of the full-length His-hP2X$_5$ construct, comprising all exon 10-specified residues plus the subsequent 12 residues of the inner half of TM2 (Fig. 4). Overall, alanine block mutations were well tolerated. Only one of the mutants, ^{330}AA^{331}-hP2X$_5$, was more likely to aggregate than to homotrimerize (Fig. 4*A*, *lane 3*). The ATP-gated inward current amplitude was similarly reduced to ~one-third of that mediated by the WT hP2X$_5$ receptor (Fig. 4*B*, *lane 3*). Cell surface radioiodination verified that the ^{330}AA^{331}-hP2X$_5$ mutant appeared exclusively as properly assembled trimers at the surface, albeit at lower levels than the WT hP2X$_5$ receptor (Fig. 4*C*). Strikingly, none of the penta-alanine block mutations covering the entire span of TM2 affected either subunit homotrimerization (Fig. 4*A*) or export to the plasma membrane (Fig. 4, *B* and *C*). Robust inward cur-

FIGURE 2. **Contribution of exon 10-encoded residues to hP2X$_5$ subunit assembly and function.** *A*, topology model of the full-length hP2X$_5$ subunit. The indicated location of the transmembrane segments TM1 (residues 29–51) and TM2 (residues 340–362) is based on the topology prediction programs MEMSAT2.0 (59) and TMHMM2.0 (60), which predicted identical boundaries for both transmembrane segments. Exon 10-encoded residues are labeled in *blue*. The N-terminal hexahistidine tag (*green*) and 2 *N*-glycans in positions Asn^{77} and Asn^{202} of the ectodomain are also indicated. The topology map was drawn with TeXtopo (61). *B*, migration on blue native PAGE gels of various P2X$_5$ receptor constructs (for sequences see *bottom panel*) isolated after overnight [^{35}S]methionine labeling. Where indicated, samples were partially denatured with 0.1% SDS (1 h at 37 °C). *C*, oligomeric state *versus* electrophysiological function. *Upper panels* show quantitative scans of the indicated lanes of the blue native PAGE gel of *B* to display the relative amounts of homotrimers and aggregates. *Lower panels* show representative current traces elicited by 1 mM ATP (denoted by *gray areas*) in oocytes expressing the same hP2X$_5$ construct as those for which the oligomeric assembly state is shown in the adjacent *upper panel*. *D*, homotrimeric hP2X$_5$ assemblies appear at the cell surface. The indicated P2X proteins were purified from surface-radioiodinated oocytes and resolved on a blue native PAGE gel. hP2X$_5$ homodimers (visible at higher intensity amplification) and monomers (*lane 5*) were produced by weakening of non-covalent subunit interactions with 0.1% SDS (1 h at 37 °C).

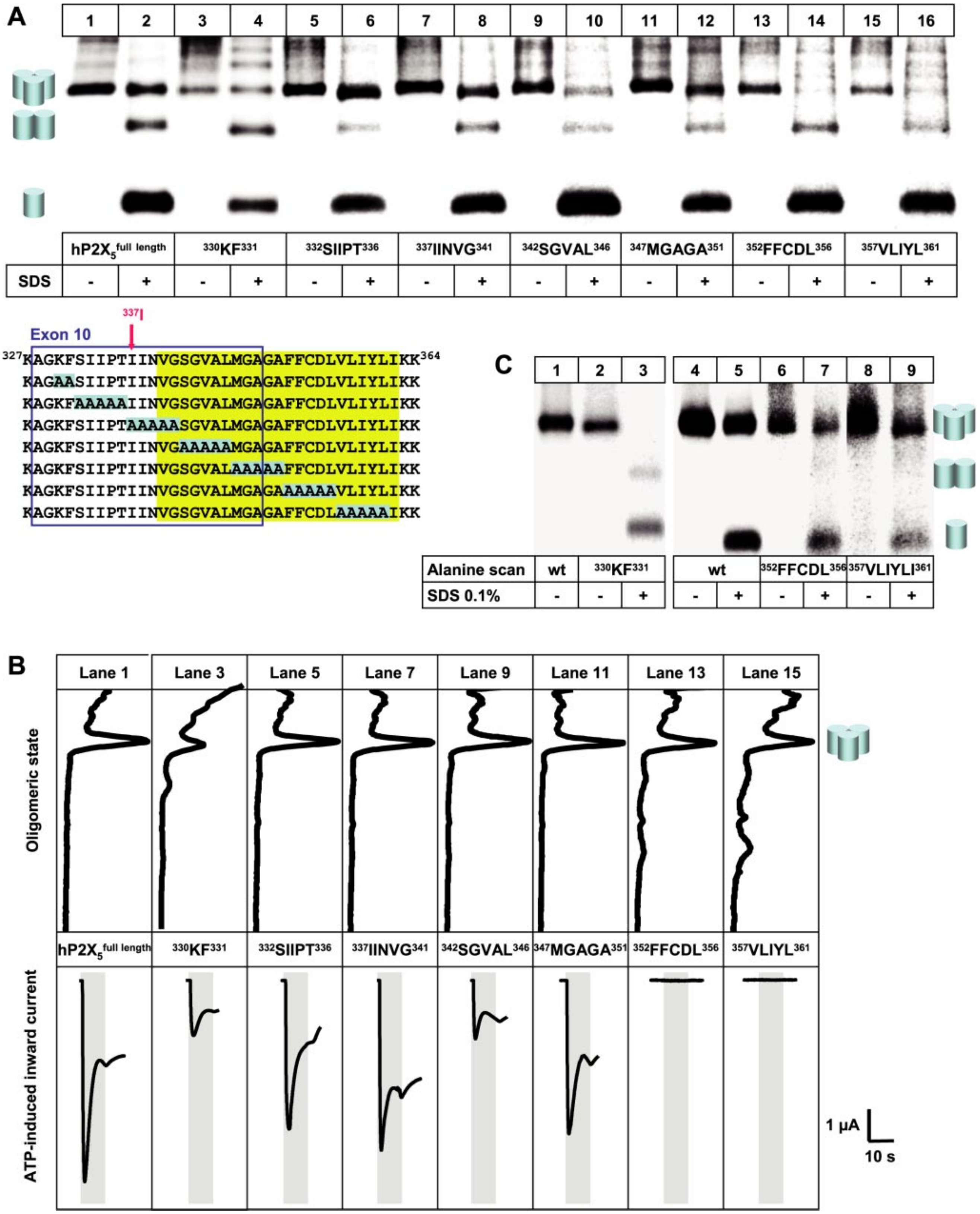

FIGURE 4. **Assembly and electrophysiological functioning of alanine-scanning mutants of pre-TM2 and TM2 regions of the hP2X$_5$ subunit.** *A*, *bottom panel*, TM2 residues are *highlighted* in *yellow*, and WT residues mutated as a whole to alanines are indicated by *gray boxes*. *Superscript numbers* refer to amino acid positions of the full-length WT-hP2X$_5$ subunits. *Top panel*, PhosphorImager scan of the indicated [^{35}S]methionine-labeled and natively purified hP2X$_5$ proteins resolved on a blue native PAGE gel. WT residues replaced as a whole by alanines are indicated. Where indicated, proteins were partially denatured by 0.1% SDS (1 h at 37 °C). Note that all hP2X$_5$ alanine replacement mutants migrated as homotrimers. *B*, oligomeric state *versus* electrophysiological function. *Top panels* and *bottom panels* show quantitative scans of the indicated lanes of the blue native PAGE gel of *A* and representative current traces elicited by 1 mM ATP (denoted by *gray areas*), respectively, from oocytes expressing the same hP2X$_5$ mutants. *C*, both electrophysiologically functional and non-functional alanine replacement mutants appear as homotrimers at the cell surface. The indicated proteins were purified from surface-radioiodinated oocytes, resolved on a blue native PAGE gel, and visualized by PhosphorImager scanning.

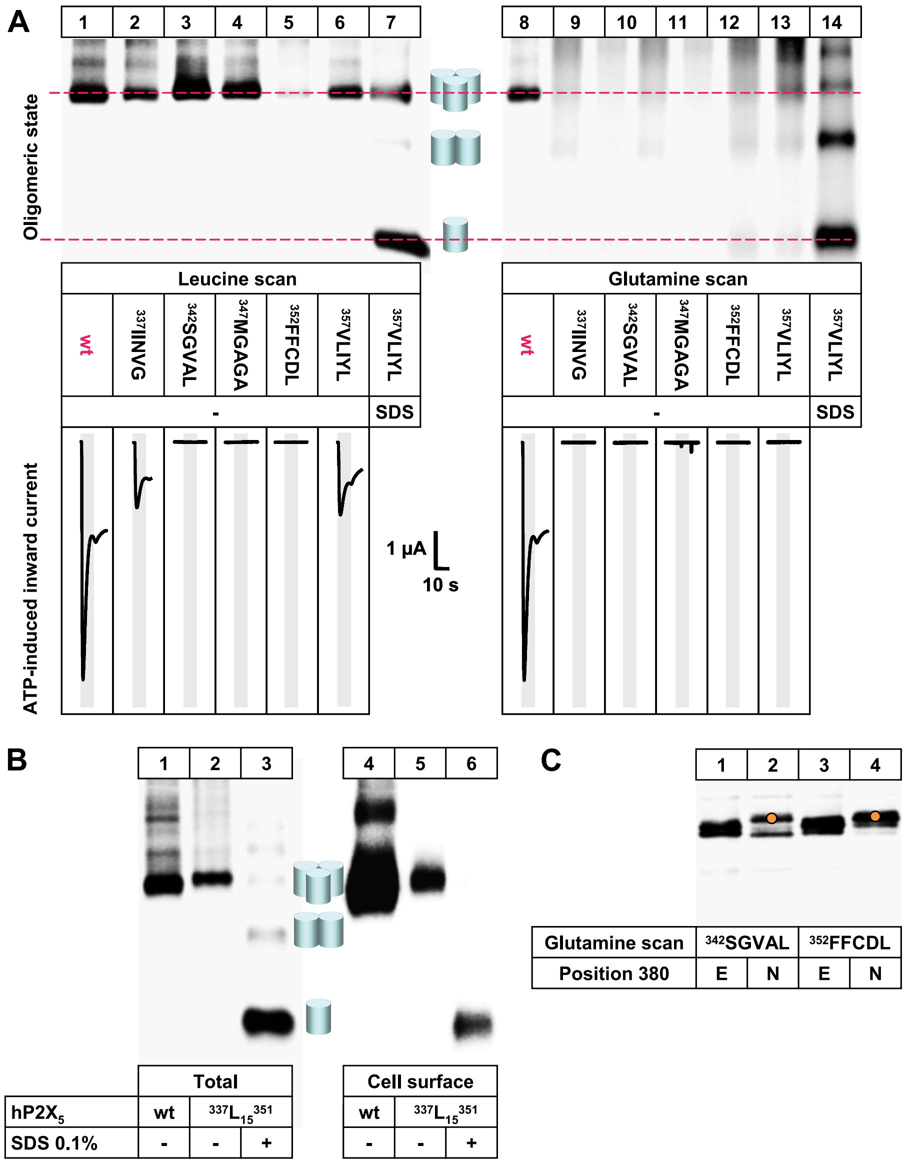

FIGURE 5. **Oligomeric state and electrophysiological functioning of penta-leucine and penta-glutamine scanning mutants of the TM2 region of the hP2X$_5$ subunit.** The initial residue of the TM2 scan, Ile^{337}, is indicated by a *red arrow* in the *bottom panel* of Fig. 3*A*. *A*, PhosphorImager scan of [^{35}S]methionine-labeled and natively purified hP2X$_5$ proteins resolved on a blue native PAGE gel. WT residues replaced as a whole by leucines or glutamines are indicated. *Bottom panels* show representative current traces elicited by 1 mM ATP (denoted by *gray areas*) from oocytes expressing the same hP2X$_5$ mutants. *B*, as a whole substitution of 15 consecutive TM2 residues (337–351) by leucines did not impair homotrimer formation. *Total* and *Cell surface* refer to the [^{35}S]methionine-labeled total protein (both surface and intracellular) and the ^{125}I-labeled surface form of the protein, respectively. Where indicated, proteins were partially denatured by 0.1% SDS (1 h at 37 °C). *C*, glutamine block mutations prevent formation of a second transmembrane domain. Glutamine mutants bearing an engineered glycosylation reporter site (Asn^{380}, *cf.* model in Fig. 3*B*) instead of the WT Glu^{380} residue migrate as triply glycosylated protein bands (*orange dot*) in the SDS-PAGE gel, indicating luminal location of the C-terminal tail.

rents in response to ATP were mediated by most of the mutants. Only penta-alanine substitutions in the inner third of TM2 (residues 352–361) abolished channel function, but these mutants also appeared as homotrimers at the cell surface (Fig. 4, *B* and *C*).

To examine if trimer formation is also possible when bulkier residues than alanine are substituted, we performed a similar mutagenesis of TM2 with penta-leucine and penta-glutamine substitutions. Results obtained by leucine replacements of residues 337–361 resembled those obtained by equivalent alanine replacements except in one respect; the ^{352}FFCDL mutant trimerized only weakly (Fig. 5*A*, *lane 5*). All the other leucine replacement mutants assembled into homotrimers as efficiently (*lanes 2–4* and *6*) as the parent hP2X$_5$ subunit (*lane 1*). Even when 15 consecutive residues constituting the N-terminal two-thirds of TM2 (residues 337–351) were simultaneously replaced by leucines, homotrimers formed and appeared at the cell surface (Fig. 5*B*). However, inclusion of the ^{352}FFCDL sequence to replace 20 consecutive residues by leucines virtually abolished trimer formation (results not shown). Responses to ATP could be elicited from mutants carrying leucine replacements at the membrane entry (residues 337–341) or exit sites of TM2 (residues 357–361), but penta-leucine replacements in the center of TM2 resulted in nonfunctional trimers (Fig. 5*A*, *lanes 1–6*, *lower panels*).

Penta-glutamine block replacements of the same TM2 residues resulted in all cases in severe assembly defects, as judged by the inability of these mutants to migrate as defined oligomers on blue native PAGE gels (Fig. 5*A*, *lanes 9–13*). Moreover, all the penta-glutamine replacement mutants were nonfunctional in terms of mediating ATP-gated inward currents (*lanes 9–13*, *lower panels*). Introducing the same glycosylation reporter sequence ^{380}NDS as described above (*cf.* Fig. 3*B*) into two of the glutamine mutants resulted in a 2–3-kDa increase in molecular mass (Fig. 5*C*). This mass shift indicates usage of Asn^{380} and, accordingly, exclusion of the penta-glutamine block-containing TM2 sequence from the membrane.

To address the impaired trimerization of the ^{352}FFCDL leucine replacement mutant in more detail, single, double, and triple mutants were generated. All of the mutants that included the D355L mutation trimerized very weakly even if singly mutated (Fig. 6*A*, *lanes 2–4*). In contrast, leucine replacement of ^{352}FFC alone, thus excluding Asp^{355}, did not lower the trimerization efficiency (Fig. 6*A*, *lane 5*). Quantification of radioactivity showed that about 10-fold fewer trimers were formed from the D355L-containing mutants than from the WT hP2X$_5$ subunit or from the ^{352}FFC leucine replacement mutant. In addition, a subset of the D355L-containing mutants

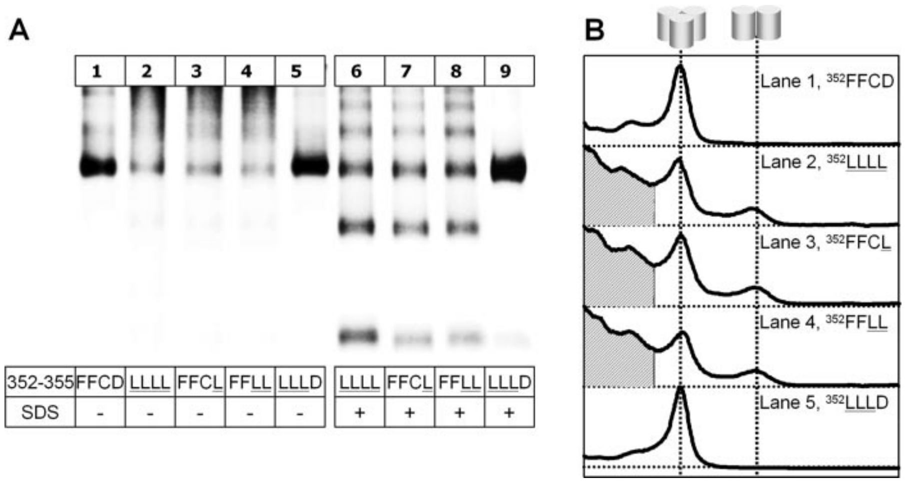

FIGURE 6. **Leucine substitution of Asp^{355}, located in TM2, greatly impairs homotrimerization.** *A*, PhosphorImager scan of [^{35}S]methionine-labeled and natively purified hP2X$_5$ proteins resolved on a blue native PAGE gel. Residues substituted in the native ^{352}FFCD sequence are *underlined*. *B*, quantitative scans of the indicated lanes of the PhosphorImager scan in *A* display the relative amounts of dimers, trimers, and aggregates (indicated by *hatched areas*).

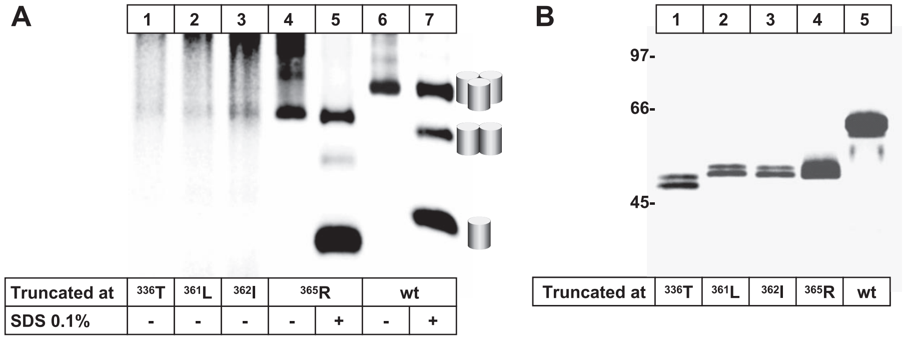

FIGURE 7. **Effect of hP2X$_5$ subunit truncation on homopolymerization.** *A*, PhosphorImager scan of a blue native PAGE gel of [^{35}S]methionine-labeled and natively purified hP2X$_5$ proteins truncated at the indicated C-terminal positions. Trimer formation required the entire TM2 and three C-terminal basic residues, ^{363}KKR^{365}, the positions of which are marked by *red arrows* in the topology model in Fig. 2*A*. *B*, PhosphorImager scan of a reducing SDS-PAGE gel of the same samples as in *A*.

migrated as dimers. This can best be seen in the quantitative scans of the various protein lanes (Fig. 6*B*). None of these mutants was capable of mediating ATP-gated inward current in oocytes, as assessed by two-electrode voltage-clamp measurements.

The Entire TM2 Domain Is Required for Subunit Trimerization—To further examine the role of TM2 in subunit trimerization, we generated truncated forms of the full-length hP2X$_5$ subunit by inserting premature stop codons at C-terminal positions which excluded or included TM2 or portions thereof. Blue native PAGE showed that trimerization occurred only when the expressed polypeptide comprised the entire TM2, capped by three basic residues, ^{363}KKR^{365}, at the extreme C-terminal end (Fig. 7*A*). Analysis of equivalent samples under denaturing conditions on a reducing SDS-PAGE gel verified that all truncation mutants were expressed with the expected molecular masses (Fig. 7*B*).

Assembly-competent TM2 Mutants Are as Tightly Folded as the WT hP2X$_5$ Receptor—The WT hP2X$_5$ subunit has 33 lysine and 24 arginine residues, potential cleavage sites for trypsin. The 61-kDa subunits of the non-denatured trimeric WT hP2X$_5$ receptor were cleaved at the lowest trypsin concentration to yield two major products of 57 and 51 kDa (Fig. 8*A*, *lane 2*). These fragments arose evidently from proteolytic removal of the cytoplasmic N and/or C-terminal tails, which have calculated masses of 3.1 and 9.0 kDa, respectively. The 51-kDa fragment was still prominent at a 10-fold higher trypsin concentration (*lane 3*). At a 100-fold higher trypsin concentration (*lane 4*), extensive digestion occurred, with a 17-kDa band being the predominant species. In contrast, two mutants judged as completely assembly-incompetent by blue native PAGE (*cf.* Figs. 5*A* and 7*A*) were degraded almost to completion even at the lowest trypsin concentration used (Fig. 8*A*, *lanes 5–12*). The site of initial proteolytic scission of a native protein is mainly determined by its higher order structure and much less by its primary sequence (27). We, therefore, deduced from these results that particularly the ectodomain of the WT hP2X$_5$ receptor must be tightly folded to resist full digestion by a trypsin concentration sufficient to completely digest aggregated hP2X$_5$ polypeptides. This result further suggests that hP2X$_5$ polypeptides contained in aggregates exist in a substantially unfolded state.

Next, we systematically tested the trypsin susceptibility of five leucine replacement mutants that cover the entire TM2 region and that all assembled as trimers, although with distinct differences in efficiency. Three of the mutants covering Ser^{342}–Leu^{356} were non-functional. Under identical digestion conditions, identical patterns of tryptic fragments were produced from the WT hP2X$_5$ receptor (Fig. 8*B*, *lanes 1–4*) and from both the functional (*lanes 5–8* and *21–24*) and non-functional mutants (*lanes 9–20*).

The initial proteolytic events are the most critical for unraveling structural features, since proteins fragments are more easily degraded as a result of their enhanced flexibility than the intact protein (27). Therefore, we quantified trypsin resistance of TM2 mutants by relating the amount of the two major products formed at the lowest trypsin concentration to the amount of the non-trypsin-treated intact polypeptide. Non-functional leucine replacement mutants were as resistant to trypsin digestion as either the WT hP2X$_5$ receptor or the functional mutants (Fig. 8*C*). The TM2 mutants that contained a D355L exchange, although exhibiting ~10–15% trypsin resistance, were proteolyzed to a markedly greater extent than the other mutants (Fig. 8, *B*, *lanes 17–20*, and *C*). As shown above, the mutants harboring D355L existed mostly as aggregates and less as trimers (*cf.* Fig. 6). Accordingly, the intense non-trypsin-treated polypep-

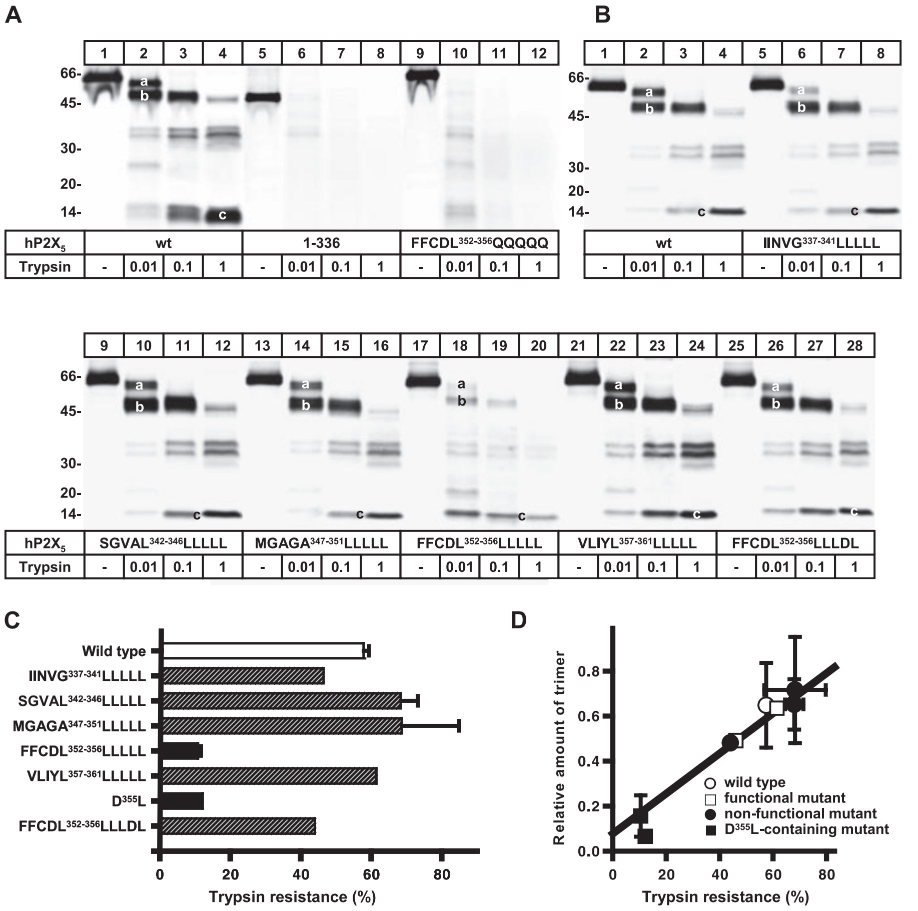

FIGURE 8. **Probing the structure of P2X$_5$ receptor mutants by limited proteolysis.** Proteolysis was carried out on the purified non-denatured hP2X$_5$ receptor and its mutants at the indicated trypsin concentrations (in mg/ml) for 15 min at 4 °C. *A* and *B* show PhosphorImager scans of reducing Tricine SDS-PAGE step gels (10%/16% acrylamide). The positions of molecular mass markers (in kDa) are shown on the *left* of each *panel*. *a*, *b*, and *c* indicate major proteolytic fragments of 57, 51, and 17 kDa, respectively, of the 61-kDa intact hP2X$_5$ subunit. *A*, trimerization-incompetent P2X$_5$ receptor mutants are highly trypsin-sensitive. *B*, trimerization-competent P2X$_5$ receptor mutants exhibit trypsin resistance comparable with the WT hP2X$_5$ receptor. *C*, quantification of trypsin resistance. The trypsin resistance of the indicated P2X$_5$ receptor constructs was expressed as the percentage of radioactivity incorporated in the two bands *a* and *b* after 0.01 mg/ml trypsin treatment relative to that detectable in the corresponding intact P2X$_5$ polypeptide of the non-trypsin-treated sample. Data are from *B* except for the additional D355L-hP2X$_5$ single mutant, which was analyzed on a separate gel not shown. *Filled columns*, D355L-containing mutants. *D*, relationship between trimerization efficiency and trypsin resistance. Trypsin resistance data are from *C*. The relative amount of trimers was calculated for equivalent samples by normalizing the radioactivity incorporated into trimers as resolved on blue native PAGE gels to the radioactivity of the corresponding monomer resolved by Tricine SDS-PAGE (from *B*). Data of the D355L-hP2X$_5$ mutant not included in *B* are also shown. In *C* and *D*, *error bars* indicate S.D. values of duplicate determinations; where absent, single determinations are shown.

tide band in the SDS-PAGE gel (Fig. 8*B*, *lane 17*) originates predominantly from aggregates and much less from trimers. Because trypsin treatment rapidly degrades hP2X$_5$ mutants contained in aggregates, the weak bands that are left (*lane 18*) must originate from the small fraction of trimers, which apparently resisted degradation.

The important contribution of Asp^{355} to efficient trimerization and, accordingly, to overall trypsin resistance is also apparent from a leucine block mutant that explicitly retained Asp^{355} (Fig. 8*B*, *lanes 25–28*). The strong increase in trimer formation (*cf.* Fig. 6) was accompanied by an equivalent increase in trypsin resistance (Fig. 8*C*).

To further strengthen our view that trimers represent the trypsin-resistant entity, we plotted the amount of trimers (normalized to monomers) against trypsin resistance (Fig. 8*D*). Data points originating from functional and non-functional mutants are both located on one straight line. Linear regression analysis yielded a significant correlation ($r = 0.76$, $p < 0.0001$), indicating that trypsin resistance refers indeed to the fraction of P2X$_5$ polypeptides that are assembled as trimers. The close relationship suggests further that the overall folding of the WT hP2X$_5$ receptor and all the TM2 mutants studied must be very similar if not identical.

DISCUSSION

P2X subunits trimerize cotranslationally in the endoplasmic reticulum and reside in intracellular compartments and in the plasma membrane as permanently assembled trimeric receptor complexes (2) (“obligomers” (28)). Here we investigated the contribution of residues encoded by exon 10 and of the subsequent residues in TM2 to hP2X$_5$ subunit trimerization. We demonstrated that the hP2X$_5^{\Delta 328-349}$ splice variant forms aggregates instead of trimers, indicating that a severe defect in assembly is one reason for the known inability of this polypeptide to form functional ATP-gated receptors (8, 9). Consistent with the view that the absence of a defined trimeric state on the blue native PAGE gel in general reflects a non-native conformation of a P2X receptor, aggregated hP2X$_5$ proteins, including the hP2X$_5^{\Delta 328-349}$ splice variant, were entirely retained in the endoplasmic reticulum by the quality control system. Moreover, structural probing by limited proteolysis revealed an extreme trypsin susceptibility of aggregates that is consistent with the view that aggregates consist of essentially unfolded polypeptides.

In contrast, trimerization-competent constructs, as judged by blue native PAGE, exhibited substantial trypsin resistance in the native state and were all exported to the cell surface. The virtually identical degree of resistance to trypsin digestion of the WT hP2X$_5$ receptor and the assembly-competent functional and non-functional mutants indicates that they all share a similar tightly folded structure. The presence of a trimeric state was not necessarily equivalent with an electrophysiologically functional receptor, as indicated by trimerization-competent hP2X$_5$ constructs that incorporated only 11 or 14 residues from the total of 22 exon 10-encoded residues. These polypeptides appeared at the cell surface exclusively as fully assembled trimers but were unable to mediate an ATP-gated current.

TM2 Plays an Indispensable Scaffolding Role in P2X$_5$ Subunit Homotrimerization—An involvement of TM2 in the assembly of P2X receptors has previously been inferred from co-immunoprecipitation assays (7). A P2X$_2$ deletion mutant terminating 25 amino acids N-terminal to TM2 did not co-precipitate with other subunits or with itself, suggesting that the missing region of the protein participates in assembly. In contrast, a truncation located C-terminal to TM2 at position Tyr^{362} of the P2X$_2$ subunit (corresponding to Tyr^{368} of P2X$_5$) enabled co-isolation. These and additional data obtained by studies of chimeras led to the conclusion that TM2 is a critical determinant for productive P2X subunit assembly (7).

Our present data offer a substantially extended perspective on this issue by showing that TM2 contributes to assembly first of all merely as a hydrophobic membrane anchor rather than by providing specific subunit recognition information. This conclusion is supported by the following data. First, blocks of five consecutive amino acid residues could be replaced by alanines throughout the entire pre-TM2 and TM2 regions without impairing homotrimer formation. Second, the absence of the outer half of TM2 residues did not prevent efficient homotrimeric assembly if a sufficiently long alanine stretch was present in the pre-TM2 region in order to alleviate the hydrophobic mismatch, thus enabling formation of a second membrane-spanning segment. Third, all sequence manipulations that prevented the formation of a second membrane-spanning segment also led to subunit aggregation and accelerated protein degradation. This was true for the exon 10-lacking hP2X$_5^{\Delta 328-349}$ variant, for a series of pre-TM2 and TM2 mutants with original residues replaced by blocks of polar residues (serines or glutamines), and for C-terminal truncation mutants, which included all pre-TM2 and TM2 residues but lacked a positively charged cap, ^{363}KKR^{365}, at their free C-terminal end. In summary, we note a close relationship between correct lipid bilayer insertion of a hydrophobic domain in N$_{exo}$-C$_{cyt}$ orientation and proper P2X$_5$ subunit trimerization.

P2X$_5$ Subunit Assembly Is Not Driven by Specific Packing Interactions of TM2 Residues—Major driving forces for association of helices in membrane proteins are (i) van der Waals interactions such as those mediated by the membrane-spanning leucine zipper domain (29) or the abundant G*XXX*G motif of bitopic proteins (30) and (ii) hydrogen bonding between polar residues. TM domains of P2X receptors do not contain a leucine zipper-like motif, but small residues (Gly, Ala, Ser) are over-represented in the outer half of TM2 of all P2X subunits and may allow for tight van der Waals packing between neighboring helices. The outer TM2 half of the hP2X$_5$ subunit contains as many as 8 small residues (4 Gly, 3 Ala, 1 Ser) over a span of 11 residues. Of these, the sequence ^{340}V$\underline{\text{G}}$SGV$\underline{\text{A}}^{345}$ ($\underline{\text{G}}$*XXX*$\underline{\text{A}}$) is reminiscent of the common pattern defined by the G*XXX*G-containing assembly motif of glycophorin A; small residues are next to the larger side chains of the β-branched amino acids valine and isoleucine (31), enabling strong (SDS-resistant) self-association by a ridge-into-groove mode of packing (32). However, in contrast to the exquisite specificity of TM-mediated dimerization of glycophorin A, which is destabilized significantly by small interfacial changes (33–35), homotrimerization of hP2X$_5$ subunits was entirely insensitive to such mutations. Even when 15 consecutive TM2 residues, Ile^{337}–Ala^{351}, including all eight small residues, were mutated to leucines, homotrimerization was unimpaired. Pure polyleucine-based coiled-coil helices mediate only relatively weak associations betweens TM domains in the absence of a polar residue (36). Thus, despite the fact that small residues occur abundantly in helix interfaces of membrane proteins and mediate tight helix-helix interactions (37), small residues in TM2 are not necessary for efficient P2X$_5$ subunit trimerization.

Intramembrane Hydrogen Bonding May Play a Role in Initiation of Homotrimerization—hP2X$_5$ homotrimer formation was remarkably tolerant to TM2 substitutions by small (alanine) and large (leucine) residues except in one position, Asp^{355}, which represents the only charged TM2 residue. Recent evidence indicates that single strongly polar residues (Asp, Asn, Glu, Gln) in a transmembrane helix can be sufficient to drive self-association of transmembrane helices through the formation of side-chain/side-chain interhelical hydrogen bonds in the absence of detailed packing (36, 38–40). The importance of Asp^{355} and, accordingly, of hydrogen bonding as a hotspot in P2X$_5$ subunit assembly is limited insofar as that (i) the D355L mutation reduced, but did not abolish hP2X$_5$ subunit homotrimerization, and (ii) substitution of Asp^{355} by alanine did not impair homotrimerization. To account for these observations, we propose that Asp^{355}, by satisfying hydrogen bonding groups in the membrane, functions at an early stage of the assembly process (41) to drive intersubunit interactions to form higher order oligomers. A locally increased effective subunit concentration may provide an environment that promotes interactions between specific assembly interfaces, which are evidently located in the ectodomain. This model can explain the observation that Asp^{355} increases the yield of homotrimers during biosynthesis but is not essential for the continued structural maintenance of the fully assembled homotrimer. Admittedly, the undisturbed assembly of the D355A mutant cannot be directly integrated in this model, and additional experiments are needed to assess the extent to which intramembrane hydrogen bonding contributes to hP2X$_5$ subunit homotrimerization.

Negative Hydrophobic Mismatch Results in hP2X$_5$ Subunit Aggregation—The inability of the splice variant hP2X$_5^{\Delta 328-349}$ to form a second membrane-spanning domain can be directly attributed to the absence of the exon 10-encoded pre-TM2 region and to the absence of the outer half of TM2. Using a helix translation of 1.5 Å per residue, the calculated hydrophobic length of the existing inner half of TM2, ^{350}GAFFCDLVLIYLI^{362}, is ~20 Å, which is clearly too short to span the 30-Å hydrophobic core of the membrane. Studies with synthetic hydrophobic peptides consisting of a polyleucine or polyleucine/alanine hydrophobic stretch have demonstrated that helices too short to span the phospholipid model membranes (referred to as negative hydrophobic mismatch) are excluded from the lipid bilayer. Because of the general insolubility of hydrophobic segments in the aqueous phase, peptides with a negative hydrophobic mismatch have a strong tendency to aggregate (42, 43). Proteins such as bacteriorhodopsin (44,

45) and Ca^{2+} ATPase (46) behave in a similar fashion and aggregate when reconstituted in phospholipids with short chain fatty acids; the excluded hydrophobic helices are shielded by self-association from the energetically unfavorable contact with the aqueous solvent. By analogy, we suggest that the hydrophobic mismatch-induced exclusion of incomplete TM2 segments from the lipid bilayer accounts for the propensity of the TM2-defective mutants to aggregate.

The support of TM2 formation and, hence, subunit trimerization by a polyalanine sequence inserted in the exon 10-lacking splice variant deserves comment. Alanine exhibits a high propensity for α-helical conformations, but the hydrophobicity of lysine-flanked polyalanine peptides is just at the threshold required for transmembrane integration into pure lipid bilayers (47). However, introduction of a few leucines into a polyalanine scaffold is sufficient to stabilize an exclusively transmembrane orientation (48). Similarly, a stretch of 16 alanines and 5 leucines was determined as the threshold value of hydrophobicity required to function as a stop-transfer sequence and to anchor alkaline phosphatase, a water-soluble protein, in *Escherichia coli* membranes (49). We suggest that the highly hydrophobic inner half of TM2 is capable of compensating for the weak or absent hydrophobicity of inserted polyalanine blocks to keep the overall hydrophobicity above the threshold for stable membrane insertion.

P2X$_5$ Homotrimerization Is Further Supported by Residues That Anchor TM2 in the Cytoplasmic Membrane-Water Interface—Truncation of the full-length P2X$_5$ subunit C-terminal to the entire TM2 region also resulted in aggregation as long as the C-terminal tail of the hydrophobic segment was not flanked by the naturally occurring residues ^{363}KKR^{365}. Positive charges in the region flanking a transmembrane segment are known to represent topological determinants that tend to have cytoplasmic localizations (50). Moreover, flanking lysine residues are thought to electrostatically anchor the position of the edge of a TM helix in the acidic phospholipid head-group region of the membrane-water interface, thus securing a stable transmembrane orientation of the helix more or less perpendicular to the bilayer surface (51). The importance of flanking lysine residues as anchors for a stable transmembrane orientation is particularly obvious in experiments with synthetically designed transmembrane peptides, which also show that basic flanking residues disfavor extensive peptide aggregation (52). Interestingly, sufficiently long hydrophobic peptides that are flanked by lysine residues only at the C-terminal end have the peculiar feature of spontaneously adopting a transmembrane orientation (53). Overall, several mechanisms may account for the crucial role of the ^{363}KKR^{365} sequence in the assembly of C-terminal-truncated P2X$_5$ subunits. However, within the context of the full-length P2X$_5$ subunit, the ^{363}KKR^{365} sequence appears of limited importance for assembly.[4]

TM2 Side-chain Chemistry and Channel Function—A detailed characterization of the electrophysiological properties of the various P2X$_5$ mutants was beyond the scope of the present study, and thus, only maximum current amplitudes elicited by a supersaturating concentration of ATP (1 mM) were recorded. hP2X$_5$ channel function was not abolished by penta-alanine substitutions in the outer half of TM2 (as summarized in the model in Fig. 9) even when the sole non-hydrophobic residue of this region, Ser^{342}, was also replaced by alanine. Most of this tolerant region bears small residues including glycine, so their mutation to alanine (Gly^{341}–Ala^{351}) caused only moderate changes in side-chain volume. Block substitutions by penta-leucines were less well accommodated and ablated function except at the outer and inner end of TM2 (^{337}IINVG^{341} and ^{357}VLIYL^{361}), where bulky hydrophobic residues (Ile, Leu, Val) already prevailed in the WT sequence. Apparently, small side chains are important in the center of TM2. Of these, Gly^{342} or Gly^{344} has been suggested to constitute a part of the channel gate (54), similar to the glycine hinge of K$^+$ channels (55). Smooth helical faces that result from having small interfacial residues may provide the flexibility needed for the conformational change in the center of TM2 (56) or, alternatively, may ensure a wide pathway through the channel for ions to reach the selectivity filter.

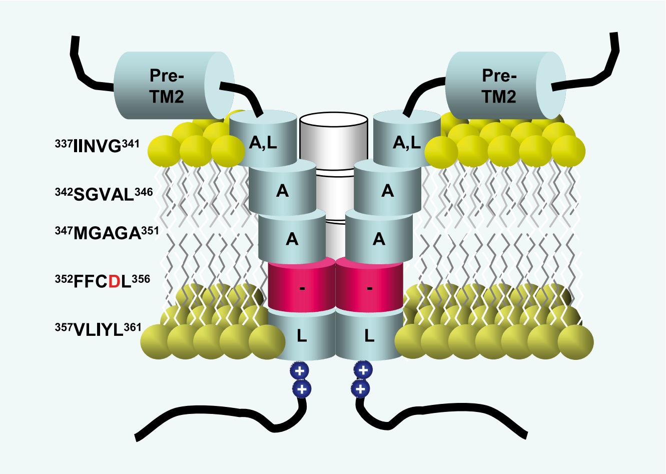

FIGURE 9. **Schematic summarizing the functional consequences of block mutations covering TM2.** Each *cylinder* corresponds to a block of five amino acid residues, the sequence of which is indicated in the *left margin*. Labeling of cylinders with *A* and/or *L* signifies that the corresponding penta-alanine (*A*) or penta-leucine (*L*) block mutations did not abolish ATP-gated cation channel function. The sole sequence block that could be neither mutated to alanines nor to leucines is *highlighted* in *red* and includes Asp^{355}. *Plus signs* indicate positively charged residues involved in the interfacial anchoring of the C-terminal end of TM2.

The sole stretch of TM2 residues that could not be block-substituted to alanines or to leucines without abolishing function was ^{352}FFCDL^{356}. Function was also abolished when Asp^{355} was singly mutated to alanine or leucine,[4] indicating that Asp^{355} has a dual role, being both structurally and functionally important. The aspartate corresponding to Asp^{355} of the P2X$_5$ subunit is conserved among all seven P2X isoforms and has been shown by cysteine-accessibility scanning to be located on the intracellular side of the channel gate of the P2X$_2$ receptor (57). Our data fit well with those of a tryptophan-scanning study on the P2X$_4$ receptor that showed that nonfunctional mutations clustered in the inner TM2 region (58). To account for the dual structural and functional roles of Asp^{355} that emerge from our study, we propose that Asp^{355} serves to control and stabilize the positioning of inner TM2 residues during the conformational transitions that accompany channel gating.

---

[4] W. Duckwitz, R. Hausmann, and G. Schmalzing, unpublished results.

TM2 and Asp^{355} Function as Scaffolds in $P2X_5$ Subunit Assembly—Our data are most compatible with the view that TM2 makes two essential contributions to $hP2X_5$ subunit oligomerization. First, the entire TM2 domain exerts a role that seems to have its basis in constraining the spatial mobility of the polypeptide chain, when the C-terminal end of the ectodomain is tethered to the membrane to form a loop-like structure. As long as certain threshold values for the hydrophobicity and length of this domain meet the requirements for membrane insertion, homotrimerization occurs. Second, TM2 formation results in an intramembrane localization of Asp^{355}, which may initiate homooligomerization by hydrogen bond-driven transmembrane helix-helix associations. We suggest that TM2 formation and the intramembrane presentation of Asp^{355} constitute scaffolds, which drive productive assembly by assisting in the creation and correct positioning of specific recognition surfaces that are evidently located in the ectodomain.

Acknowledgments—We thank Dr. Florentina Soto for providing the $rP2X_5$ clone and Dr. Sven Sadtler for PCR cloning of the $hP2X_5$ splice variant during his Ph.D. work.

REFERENCES

1. North, R. A. (2002) *Physiol. Rev.* **82,** 1013–1067
2. Nicke, A., Bäumert, H. G., Rettinger, J., Eichele, A., Lambrecht, G., Mutschler, E., and Schmalzing, G. (1998) *EMBO J.* **17,** 3016–3028
3. Nicke, A., Rettinger, J., and Schmalzing, G. (2003) *Mol. Pharmacol.* **63,** 243–252
4. Aschrafi, A., Sadtler, S., Niculescu, C., Rettinger, J., and Schmalzing, G. (2004) *J. Mol. Biol.* **342,** 333–343
5. Barrera, N. P., Ormond, S. J., Henderson, R. M., Murrell-Lagnado, R. D., and Edwardson, J. M. (2005) *J. Biol. Chem.* **280,** 10759–10765
6. Jiang, L. H., Kim, M., Spelta, V., Bo, X., Surprenant, A., and North, R. A. (2003) *J. Neurosci.* **23,** 8903–8910
7. Torres, G. E., Egan, T. M., and Voigt, M. M. (1999) *J. Biol. Chem.* **274,** 22359–22365
8. Le, K. T., Paquet, M., Nouel, D., Babinski, K., and Seguela, P. (1997) *FEBS Lett.* **418,** 195–199
9. Bo, X., Jiang, L. H., Wilson, H. L., Kim, M., Burnstock, G., Surprenant, A., and North, R. A. (2003) *Mol. Pharmacol.* **63,** 1407–1416
10. Garcia-Guzman, M., Soto, F., Laube, B., and Stühmer, W. (1996) *FEBS Lett.* **388,** 123–127
11. Gloor, S., Pongs, O., and Schmalzing, G. (1995) *Gene* **160,** 213–217
12. Schmalzing, G., Gloor, S., Omay, H., Kröner, S., Appelhans, H., and Schwarz, W. (1991) *Biochem. J.* **279,** 329–336
13. Rettinger, J., and Schmalzing, G. (2003) *J. Gen. Physiol.* **121,** 451–461
14. Rettinger, J., Aschrafi, A., and Schmalzing, G. (2000) *J. Biol. Chem.* **275,** 33542–33547
15. Thompson, J. A., Lau, A. L., and Cunningham, D. D. (1987) *Biochemistry* **26,** 743–750
16. Schägger, H., and von Jagow, G. (1991) *Anal. Biochem.* **199,** 223–231
17. Schägger, H., Cramer, W. A., and von Jagow, G. (1994) *Anal. Biochem.* **217,** 220–230
18. Schägger, H., and von Jagow, G. (1987) *Anal. Biochem.* **166,** 368–379
19. White, M. M., and Aylwin, M. (1990) *Mol. Pharmacol.* **37,** 720–724
20. Griffon, N., Büttner, C., Nicke, A., Kuhse, J., Schmalzing, G., and Betz, H. (1999) *EMBO J.* **18,** 4711–4721
21. Büttner, C., Sadtler, S., Leyendecker, A., Laube, B., Griffon, N., Betz, H., and Schmalzing, G. (2001) *J. Biol. Chem.* **276,** 42978–42985
22. Nicke, A., Rettinger, J., Mutschler, E., and Schmalzing, G. (1999) *J. Recept. Signal Transduct. Res.* **19,** 493–507
23. Gendreau, S., Voswinkel, S., Torres-Salazar, D., Lang, N., Heidtmann, H., Detro-Dassen, S., Schmalzing, G., Hidalgo, P., and Fahlke, C. (2004) *J. Biol. Chem.* **279,** 39505–39512
24. Yernool, D., Boudker, O., Jin, Y., and Gouaux, E. (2004) *Nature* **431,** 811–818
25. Nilsson, I., and Von Heijne, G. (2000) *J. Biol. Chem.* **275,** 17338–17343
26. Killian, J. A. (1998) *Biochim. Biophys. Acta* **1376,** 401–415
27. Hubbard, S. J. (1998) *Biochim. Biophys. Acta* **1382,** 191–206
28. Ofran, Y., and Rost, B. (2003) *J. Mol. Biol.* **325,** 377–387
29. Gurezka, R., Laage, R., Brosig, B., and Langosch, D. (1999) *J. Biol. Chem.* **274,** 9265–9270
30. Russ, W. P., and Engelman, D. M. (2000) *J. Mol. Biol.* **296,** 911–919
31. Senes, A., Gerstein, M., and Engelman, D. M. (2000) *J. Mol. Biol.* **296,** 921–936
32. Mackenzie, K. R., Prestegard, J. H., and Engelman, D. M. (1997) *Science* **276,** 131–133
33. Lemmon, M. A., Flanagan, J. M., Treutlein, H. R., Zhang, J., and Engelman, D. M. (1992) *Biochemistry* **31,** 12719–12725
34. Langosch, D., Brosig, B., Kolmar, H., and Fritz, H. J. (1996) *J. Mol. Biol.* **263,** 525–530
35. Schneider, D., and Engelman, D. M. (2004) *J. Mol. Biol.* **343,** 799–804
36. Zhou, F. X., Cocco, M. J., Russ, W. P., Brunger, A. T., and Engelman, D. M. (2000) *Nat. Struct. Biol.* **7,** 154–160
37. Liu, W., Eilers, M., Patel, A. B., and Smith, S. O. (2004) *J. Mol. Biol.* **337,** 713–729
38. Choma, C., Gratkowski, H., Lear, J. D., and Degrado, W. F. (2000) *Nat. Struct. Biol.* **7,** 161–166
39. Gratkowski, H., Lear, J. D., and Degrado, W. F. (2001) *Proc. Natl. Acad. Sci. U. S. A.* **98,** 880–885
40. Zhou, F. X., Merianos, H. J., Brunger, A. T., and Engelman, D. M. (2001) *Proc. Natl. Acad. Sci. U. S. A.* **98,** 2250–2255
41. Engelman, D. M., Chen, Y., Chin, C. N., Curran, A. R., Dixon, A. M., Dupuy, A. D., Lee, A. S., Lehnert, U., Matthews, E. E., Reshetnyak, Y. K., Senes, A., and Popot, J. L. (2003) *FEBS Lett.* **555,** 122–125
42. Ren, J., Lew, S., Wang, J., and London, E. (1999) *Biochemistry* **38,** 5905–5912
43. de Planque, M. R., Goormaghtigh, E., Greathouse, D. V., Koeppe, R. E., Kruijtzer, J. A., Liskamp, R. M., de, K. B., and Killian, J. A. (2001) *Biochemistry* **40,** 5000–5010
44. Lewis, B. A., and Engelman, D. M. (1983) *J. Mol. Biol.* **166,** 203–210
45. Ryba, N. J., and Marsh, D. (1992) *Biochemistry* **31,** 7511–7518
46. Cornea, R. L., and Thomas, D. D. (1994) *Biochemistry* **33,** 2912–2920
47. Lewis, R. N., Zhang, Y. P., Hodges, R. S., Subczynski, W. K., Kusumi, A., Flach, C. R., Mendelsohn, R., and McElhaney, R. N. (2001) *Biochemistry* **40,** 12103–12111
48. Bechinger, B. (2001) *Biophys. J.* **81,** 2251–2256
49. Chen, H., and Kendall, D. A. (1995) *J. Biol. Chem.* **270,** 14115–14122
50. Von Heijne, G. (1989) *Nature* **341,** 456–458
51. Killian, J. A., and Von Heijne, G. (2000) *Trends Biochem. Sci.* **25,** 429–434
52. de Planque, M. R., and Killian, J. A. (2003) *Mol. Membr. Biol.* **20,** 271–284
53. Percot, A., Zhu, X. X., and Lafleur, M. (1999) *Biopolymers* **50,** 647–655
54. Li, Z., Migita, K., Samways, D. S., Voigt, M. M., and Egan, T. M. (2004) *J. Neurosci.* **24,** 7378–7386
55. Jiang, Y., Lee, A., Chen, J., Cadene, M., Chait, B. T., and Mackinnon, R. (2002) *Nature* **417,** 523–526
56. Curran, A. R., and Engelman, D. M. (2003) *Curr. Opin. Struct. Biol.* **13,** 412–417
57. Rassendren, F., Buell, G., Newbolt, A., North, R. A., and Surprenant, A. (1997) *EMBO J.* **16,** 3446–3454
58. Silberberg, S. D., Chang, T. H., and Swartz, K. J. (2005) *J. Gen. Physiol.* **125,** 347–359
59. Jones, D. T. (1998) *FEBS Lett.* **423,** 281–285
60. Krogh, A., Larsson, B., von, H. G., and Sonnhammer, E. L. (2001) *J. Mol. Biol.* **305,** 567–580
61. Beitz, E. (2000) *Bioinformatics* **16,** 1050–1051

$P2X_5$ Subunit Assembly Requires Scaffolding by the Second Transmembrane Domain and a Conserved Aspartate

Wiebke Duckwitz, Ralf Hausmann, Armaz Aschrafi and Günther Schmalzing

J. Biol. Chem. 2006, 281:39561-39572.
doi: 10.1074/jbc.M606113200 originally published online September 25, 2006

Access the most updated version of this article at doi: 10.1074/jbc.M606113200

Alerts:

- When this article is cited
- When a correction for this article is posted

Click here to choose from all of JBC's e-mail alerts

This article cites 59 references, 23 of which can be accessed free at
http://www.jbc.org/content/281/51/39561.full.html#ref-list-1